



TITLE:

Size-controlled in situ synthesis of metal–polymer nanocomposite films using a CO laser

AUTHOR(S):

Kashihara, Kazuhiko; Uto, Yuki; Nakajima, Takashi

CITATION:

Kashihara, Kazuhiko...[et al]. Size-controlled in situ synthesis of metal–polymer nanocomposite films using a CO laser. Polymer Bulletin 2021, 78: 6969-6981

ISSUE DATE:

2021

URL:

<http://hdl.handle.net/2433/265477>

RIGHT:

This is a post-peer-review, pre-copyedit version of an article published in 'Polymer Bulletin'. The final authenticated version is available online at: <https://doi.org/10.1007/s00289-020-03481-0>; The full-text file will be made open to the public on 13 November 2021 in accordance with publisher's 'Terms and Conditions for Self-Archiving'; This is not the published version. Please cite only the published version. この論文は出版社版ではありません。引用の際には出版社版をご確認ください。

Size-controlled in-situ synthesis of metal-polymer nanocomposite films using a CO₂ laser

Kazuhiko Kashihara · Yuki Uto · Takashi Nakajima*

Institute of Advanced Energy, Kyoto University, Gokasho, Uji, Kyoto 611-0011, Japan

Abstract

In-situ synthesis of metal-polymer nanocomposite films by irradiating a CO₂ laser for several seconds is a new alternative to fabricate metal-polymer nanocomposite films. The main features of this method are that the number density of the synthesized metal nanoparticles is very high so that the optical density easily exceeds 0.5~1.5 for the film thickness of ~200 nm, and owing to the short fabrication time and the use of non-focused laser beam, large-scale processing is possible. For this technique to be applicable for a variety of purposes an important question is how and how much we can control the film properties. In this work we demonstrate that the size and size distribution of metallic nanoparticles in the synthesized nanocomposite films can be well-controlled by the choice of the laser power and irradiation time as well as the concentrations of nanoparticle precursor. Properties of the synthesized films can be roughly understood by considering the diffusion of metallic ions, atoms, and nanoparticles in the polymer film under the elevated temperature induced by the CO₂ laser.

Keywords

silver nanoparticles; morphology; polyvinyl alcohol; nanocomposites; laser

*E-mail address: nakajima@iae.kyoto-u.ac.jp (Takashi Nakajima)

ORCID iD: <https://orcid.org/0000-0003-4136-5383>

Introduction

Nanocomposites are materials with nanometer-size materials (filler) in another material (matrix), and they are used for a variety of applications such as sensors, optics, electronics, catalysis, reinforced materials, etc. A class of nanocomposites consist of metallic nanoparticles (NPs) as a filler in a polymer matrix, and they are conveniently used for many applications [1–5].

In-situ synthesis of metal-polymer nanocomposite films have some advantages over the ex-situ one in terms of the uniformity of synthesized nanoparticles in the polymer matrix. The well-known techniques for the in-situ synthesis are the direct dispersion [6], chemical reduction [7, 8], photo reduction [9–13], microwave reduction [14], and thermal reduction [15–18]. Chemical reduction method is sometimes combined with a post-processing such as laser-irradiation [19] to alter the film property. Recently we have developed another alternative [20] for the in-situ synthesis of nanocomposite films. Our method utilizes a non-focused CO₂ laser beam to irradiate a polymer film (polyvinyl alcohol, PVA or polyethylene glycol, PEG) which contains a precursor (AgNO₃) of Ag nanoparticles. In this technique the CO₂ laser heats the substrate to promote the reduction of Ag ions in the polymer matrix on it. The advantage of our method is that the reduction speed is fast (from several seconds to a few tens of seconds) and no additional reducing agent is needed, since the polymer matrix itself serves as a reducing and stabilizing agent. Moreover, unlike the known photoreduction using a UV laser which requires the use of a well-focused laser beam down to a few tens of micron to speed up the reduction process, a very modest laser power without a focus is sufficient for the CO₂ laser reduction, and hence the large-area processing is possible. More recently we have applied the developed technique to synthesize silver-methylcellulose films to study the influence of polymer molecular weight on film properties [21]. Substrate heating with a CO₂ laser is a versatile method to fabricate functional films, and it can be used not only to promote the reduction speed of metallic ions dispersed in a polymer matrix (so-called metal-polymer nanocomposite films) but also to induce solid-state dewetting of metallic films (so-called nanostructured metallic films). Indeed, we have recently shown that the irradiation of a non-focused CO₂ laser beam onto thin metallic films for a few tens of seconds at a few W enables us to rapidly induce nanostructures in thin Au [22] and Ag films [23] with some notable differences between them.

In this paper we study the morphological and optical properties of metal-polymer nanocomposite films by systematically varying the experimental parameters such as the CO₂ laser power, irradiation time, and concentration of nanoparticle precursor to explore the possibility of size-controlled synthesis of metal-polymer nanocomposite

films using a CO₂ laser. As we will show later on in this paper, we have found that not only the laser power and irradiation time but also the concentration of nanoparticle precursor significantly influences the size and size distribution of nanoparticles, and accordingly the position and width of surface plasmon resonance. Related to this paper there are several works which report the control of size and number density of metal nanoparticles synthesized in the polymer matrix through chemical reduction [24], photoreduction [25, 26], and thermal reduction [27, 28]. Co-evaporation of metal and polymer with separate evaporators brings a convenient flexibility to control the size and shape of nanoparticles [29–31]. Similarly, co-sputtering of metal and polymer can be used to achieve the controlled synthesis of nanocomposites [32, 33].

Materials and methods

Materials

PVA (molecular weight~60,000) is purchased from Sigma-Aldrich, and silver nitrate (AgNO₃, purity 99.999 %) is purchased from Wako. All the chemicals are of reagent grade and used as purchased without any further purification.

Laser

For the synthesis of Ag-PVA films we employ a CO₂ laser at 10.6 μm (AL30P, Access Laser Co., peak power 60 W, pulse duration 100-400 μs depending on the laser power, repetition rate 2.5 kHz). Since the pulse duration is comparable to the pulse interval which is 400 μs, it is nearly in the quasi-CW mode. The CO₂ laser power is measured with a power meter (Pronto-250, Gentec-EO Co.). The laser beam diameter is ~10 mm at the position of the film with a Gaussian spatial profile. This means that the effective laser power density is different as a function of distance from the irradiation center [23]. Although it is technically possible to make the spatial profile of the laser beam to a nearly flat-top by introducing a commercial beam shaper we use the laser beam as it is in this work. Accordingly, all the data presented in this work have been taken at the irradiation center on the synthesized film where the laser power density is maximum.

Synthesis of Ag-PVA films

0.125 g of PVA is mixed with 2 mL of highly purified and deionized water at room temperature under continuous stirring for 20 min, and then it is heated to 95 °C for 45 min to completely dissolve PVA. After cooling down to the room temperature the PVA solution is mixed with a separately prepared solution which contains 0.04-0.16 g of silver nitrate and 1 mL of water. The above procedure results in the AgNO₃-PVA solution which is composed of PVA (3.8 wt.%), AgNO₃ (1.2-4.9 wt.%), and deionized water. The AgNO₃(1.2-4.9 wt%)-PVA solution is

immediately spin-coated on a microscope cover glass (borosilicate glass, 18x18x0.15mm, Matsunami Co.) at 500 rpm for 5 sec which is followed by 4000 rpm for 10 sec. The AgNO₃-PVA film is dried in air at room temperature for 30 min, and then irradiated with the CO₂ laser at the chosen laser powers and irradiation time.

Characterization

To characterize the synthesized Ag-PVA films, we employ a compact CCD spectrometer (USB2000+, Ocean Optics), and scanning electron microscope (SEM) (JSM-6500FE, JEOL) at 5 kV. For the analysis of the SEM images we employ the ImageJ software to obtain the size distribution of Ag NPs and the area fraction defined by [total surface area of NPs]/[total area of the SEM image], where the surface areas of the respective NPs are estimated by πr^2 with r being the radius of NPs. Since the thickness of the synthesized films measured by the atomic force microscopy is about 200 nm (measured by atomic force microscope (VN-8010, Keyence)), there should be no clear difference between the Ag NPs at the surface of and in the PVA matrix, and accordingly the SEM images would well represent the morphology of the synthesized Ag NPs. In order to ensure that the surface morphology observed with the SEM originates from the formation of Ag NPs, we prepare a film from the pure PVA solution (without AgNO₃), irradiate it with the CO₂ laser at 1 W for 30 sec, and take the SEM image to find that the surface is very flat without any structures.

Results and discussion

Film temperature

Before showing the results of the films we first present the temporal variation of film temperature at the different laser powers. Since our CO₂ laser is in the quasi-CW mode (i.e., pulse duration ~ pulse interval), we can conveniently use a thermocouple with a small head (~1 mm diameter) to measure the film temperature at the irradiation center as a function of time [20, 22]. The results are presented in Fig. 1 at the laser powers of 0.4, 0.5, 0.6, 0.8, and 1 W for the irradiation time of 2400 sec, respectively. The small temperature modulations arise from the fluctuation of the laser power. Upon laser irradiation the film temperature rapidly increases, and it reaches a nearly steady-state temperature in 30 sec regardless of the incident laser power. Naturally, the steady-state temperature is higher for the higher laser power. When we turn off the laser, the film temperature rapidly cools down to the room temperature (~25 °C). By recalling that the thickness of the glass substrate is 0.15 mm which is far thicker than the film itself, it is the glass substrate that mainly absorbs the CO₂ laser energy, which indirectly heats the film on it.

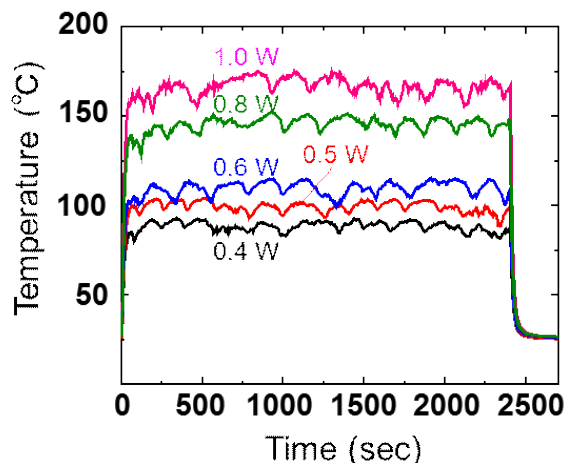


Fig. 1 Temperature change of the Ag-PVA film on a glass substrate as a function of time. In this measurement the laser power is 0.4, 0.5, 0.6, 0.8, 1 W and turned on and off at 0 and 2400 sec, respectively.

Since the boiling and thermal decomposition temperatures of bulk PVA are about 230 and 300 °C, respectively, we can say that 0.4-1 W is the appropriate range of CO₂ laser power.

Effect of the concentration of nanoparticle precursor

To start with, we study the influence of the concentration of nanoparticle precursor, i.e., AgNO₃, in the AgNO₃-PVA solutions to prepare the AgNO₃-PVA films. Those AgNO₃-PVA films are irradiated by the CO₂ laser at 1 W for 10-1200 sec. The UV-vis spectra of the synthesized Ag-PVA films are shown in Fig. 2. For the irradiation time of 10 sec the peaks of the surface plasmon resonance (SPR) are located at about 405 nm for all the concentrations of 1.2, 2.4, and 4.9 wt.%, and it is clear that Ag NPs have been formed in the PVA matrix in a much shorter time compared with the photoreduction method with a UV laser [10]. For the longer irradiation times of 120 and 1200 sec, the peaks of SPR shift to the longer wavelength side with a lift-up of the tail and the widths of the SPRs increases for all three concentrations. The shift of the peak of SPR to the longer wavelength side and the lift-up of its tail after the longer irradiation time imply the particle size increase and aggregation, respectively, while the increase of the its width means the broadened particle size distribution. This is qualitatively reasonable, since the mobilities of silver ions/ atoms/clusters/nanoparticles are higher in the heated (and hence softened) polymer matrix during the CO₂ laser irradiation at 1 W (Fig. 1), and under such situation they are more likely to meet other silver ions/atoms/clusters/nanoparticles to form larger nanoparticles through the growth or aggregation. Furthermore, for a

given irradiation time the height of the SPR is higher for the Ag-PVA films synthesized from the AgNO_3 -PVA solutions with higher concentration of AgNO_3 , and this obviously indicates that more Ag NP have been produced.

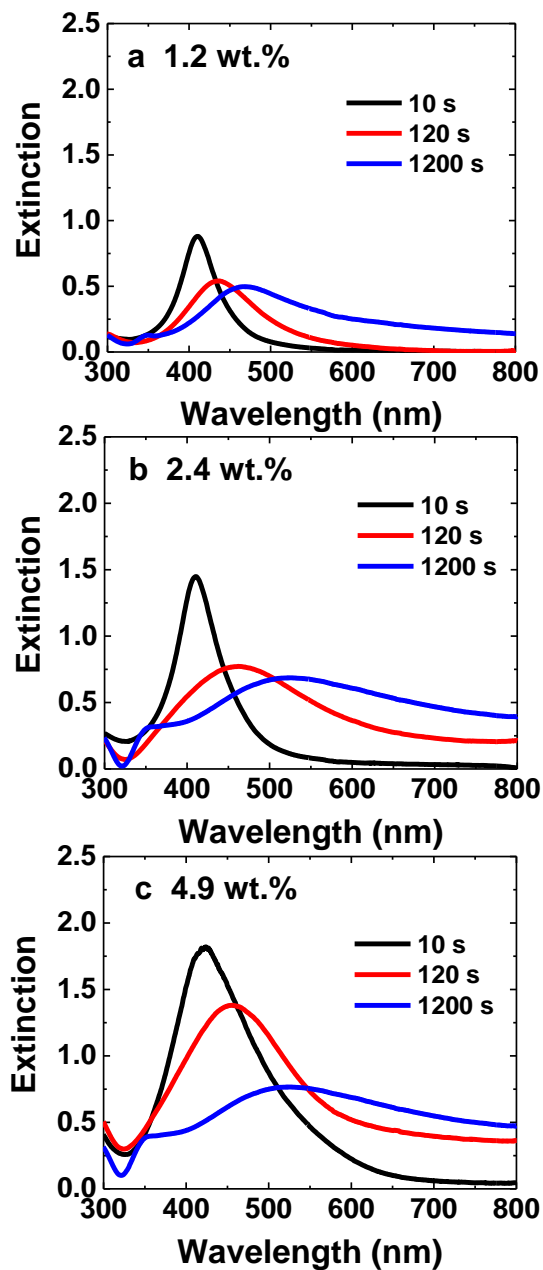


Fig. 2 UV-Vis spectra of the Ag(1.2, 2.4, and 4.9 wt.%) -PVA films synthesized from the AgNO_3 -PVA solutions with different concentrations of AgNO_3 , (a) 1.2 wt.%, (b) 2.4 wt.%, (c) 4.9 wt.%. The laser power is 1 W for all cases.

Effect of the laser irradiation time

We now fix the concentration of AgNO_3 in the solution to 4.9 wt.%, and study the effect of the laser irradiation time on the film properties. The employed laser power is 1 W and the results are summarized in Fig. 3. From Fig. 3a we notice that, although a clear SPR of Ag NPs is observed for the irradiation time of 10 s it is broadened after the 120 sec irradiation (Fig. 2c), and then the distortion becomes more severe after the irradiation times of 1200 and 2400 sec (Fig. 3a). This change implies that significant aggregation of Ag NPs takes place in the heated (and hence softened) polymer matrix during the longer irradiation time at 1 W, and this interpretation is confirmed by the SEM images shown in Figs. 3b-d. Using ImageJ we carry out the analysis of the SEM images, and obtain the size

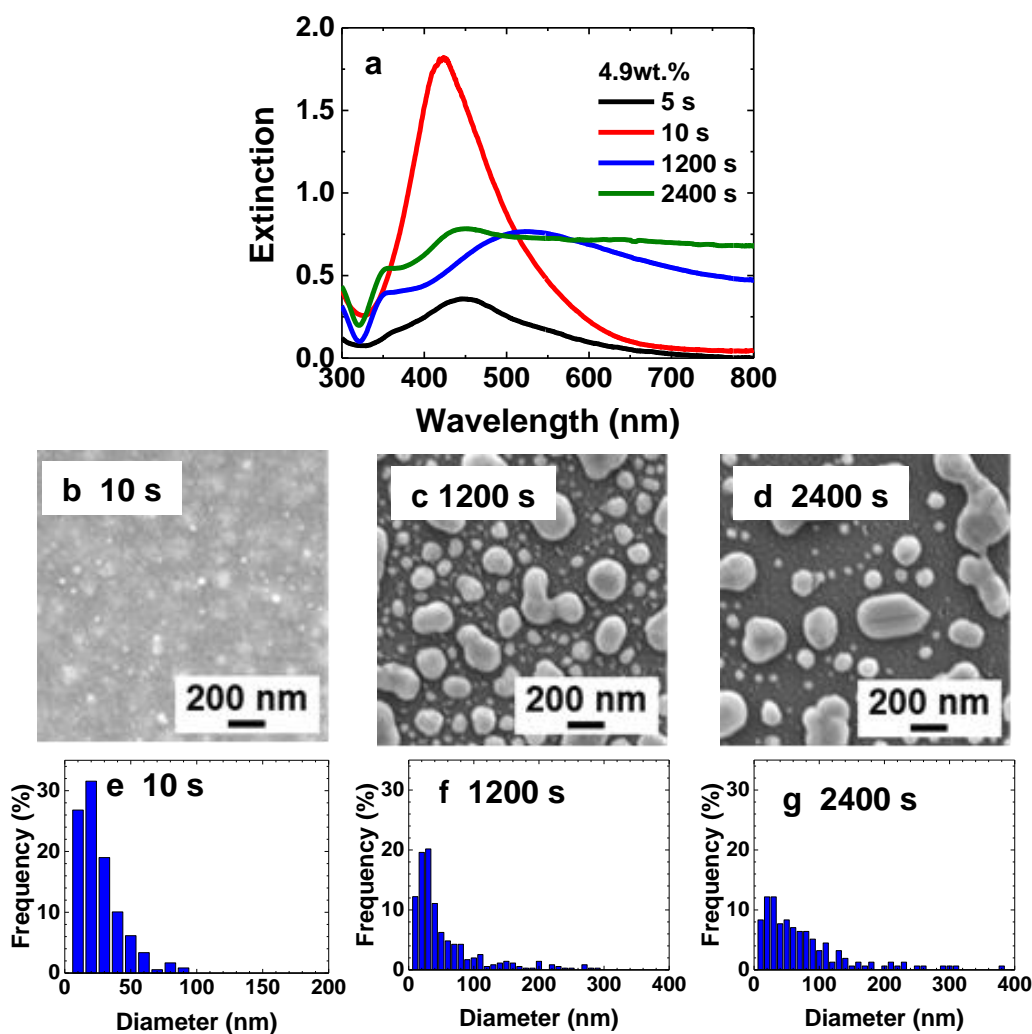


Fig. 3 (a) UV-Vis spectra, (b-d) SEM images, (e-g) histograms of nanoparticle size distribution of the Ag(4.9wt.%) -PVA films for different irradiation times (5 ~2400 s) at the laser power of 1 W.

distributions of Ag NPs after the irradiation times of 10, 1200, and 2400 sec, which are shown in Figs. 3e-g, respectively. The size of Ag NPs is relatively small and the size distribution is reasonably uniform for the irradiation time of 10 sec (Fig. 3b and e). However, for the longer irradiation times the size becomes larger and the size distribution becomes less uniform, as shown in Figs. 3c-d and Figs. 3f-g. Note that the SEM images and the size distributions in Fig. 3c, f and Fig. 3d, g, respectively, do not seem to be consistent at first glance. This is simply because a large Ag NP occupies more space in the SEM images while it is counted as one in the distribution histogram, and they are actually consistent. The most interesting feature of Fig. 3 is that the progressive change of the optical as well as morphological properties of Ag NPs synthesized at the laser power of 1 W does not seem to terminate at least until the irradiation time of 2400 sec. Presumably this is because the film temperature is sufficiently high during the laser irradiation at 1 W, and accordingly in the softened polymer matrix Ag NPs have a higher mobility to diffuse sufficient distance to meet others to aggregate.

To highlight the influence of laser power we synthesize the Ag-PVA films at the laser power of 0.5 W so that the film temperature stays below 100 °C (see Fig. 1), which means the much lower mobility of silver ions/atoms/clusters/nanoparticles in the polymer matrix at 0.5 W compared with that at 1 W. The results are summarized in Fig. 4. From the UV-vis spectra shown in Fig. 4a we notice that the peak height of SPR grows during the irradiation of first few hundred sec some blue shift [15], while it hardly changes after the 1200 sec irradiation. The SEM images and the histograms of NP size distribution shown in Figs. 4b-d and Figs. 4e-g, respectively, are consistent with the UV-vis spectra. The results at the laser power 0.5 W (Fig. 4) are in contrast to those at the laser power of 1 W (Fig. 3). This is because fewer Ag NPs are synthesized at 0.5 W, and moreover, those fewer Ag NPs can diffuse for shorter distance in the less softened polymer matrix at 0.5 W (Fig. 1), as a result of which the Ag NPs synthesized under the 0.5 W laser power hardly suffer from aggregation even during the long irradiation time. It may be interesting to investigate how the reduction, diffusion, and aggregation of NPs go when the precursor of NP is replaced from Ag (AgNO₃ in this work) to Au (say, HAuCl₄), since the formation dynamics of Ag and Au NPs have been found somehow different [34].

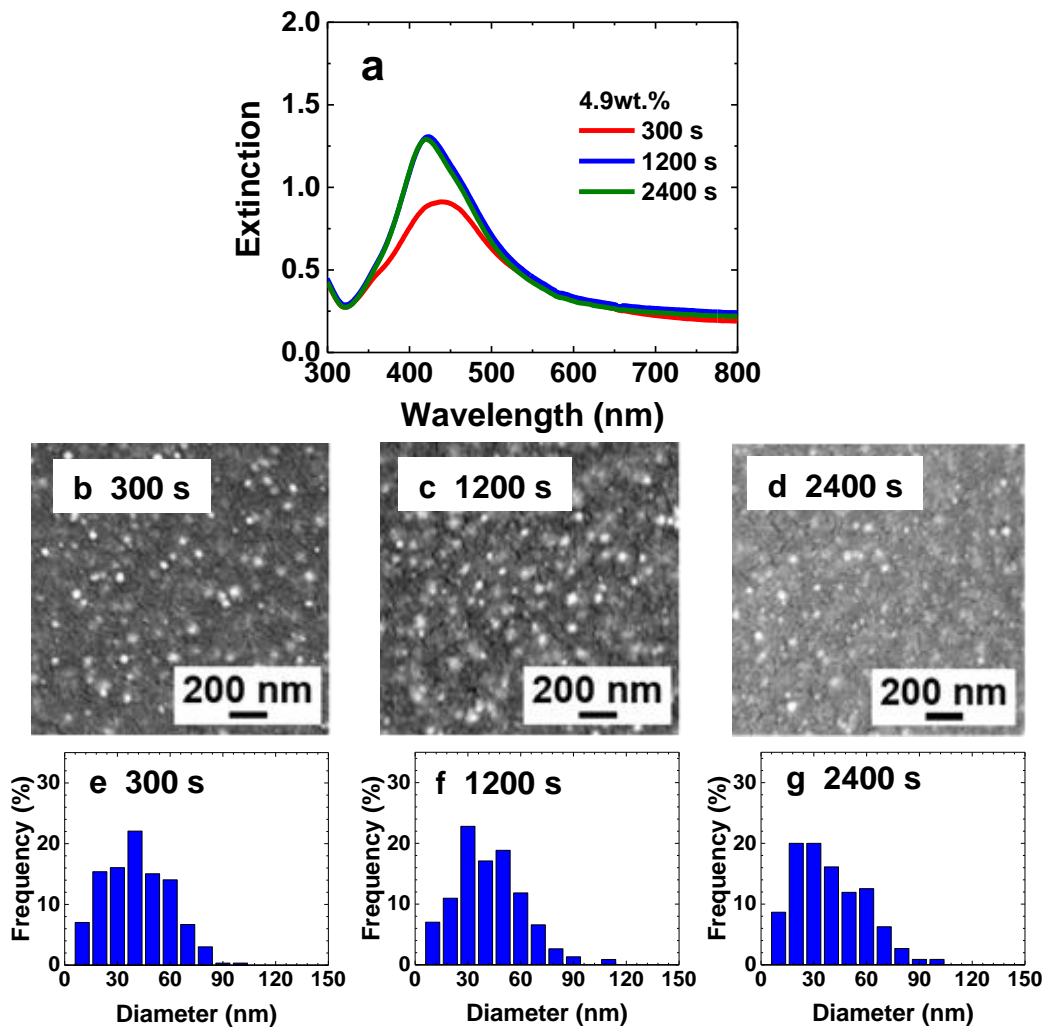


Fig. 4 Similar to Fig. 3 but at the laser power of 0.5 W.

Strategy to produce small and homogeneous Ag NPs

From the above results, we have learned that the laser power and irradiation time as well as the concentration of NP precursor (AgNO₃) strongly influence the size and shape of Ag NPs synthesized in the polymer matrix during CO₂ laser irradiation. To synthesize smaller and more uniform Ag NPs in the polymer matrix, the 0.5 W laser power seems to be safer than the 1 W laser power, since the use of 0.5 W laser power restricts the diffusion of Ag NPs in the polymer matrix to synthesize more uniform Ag NPs (Fig. 4), while a precise control of irradiation time is crucial under the 1 W laser power to synthesize small Ag NPs with minimum aggregation (Fig. 3). Moreover, we can infer from Fig. 2 that the use of lower concentration (1.2 wt%) of NPs precursor, i.e., AgNO₃ in our case, is also beneficial to synthesize small Ag NPs with minimum aggregation. Knowing all the above, we prepare the AgNO₃-

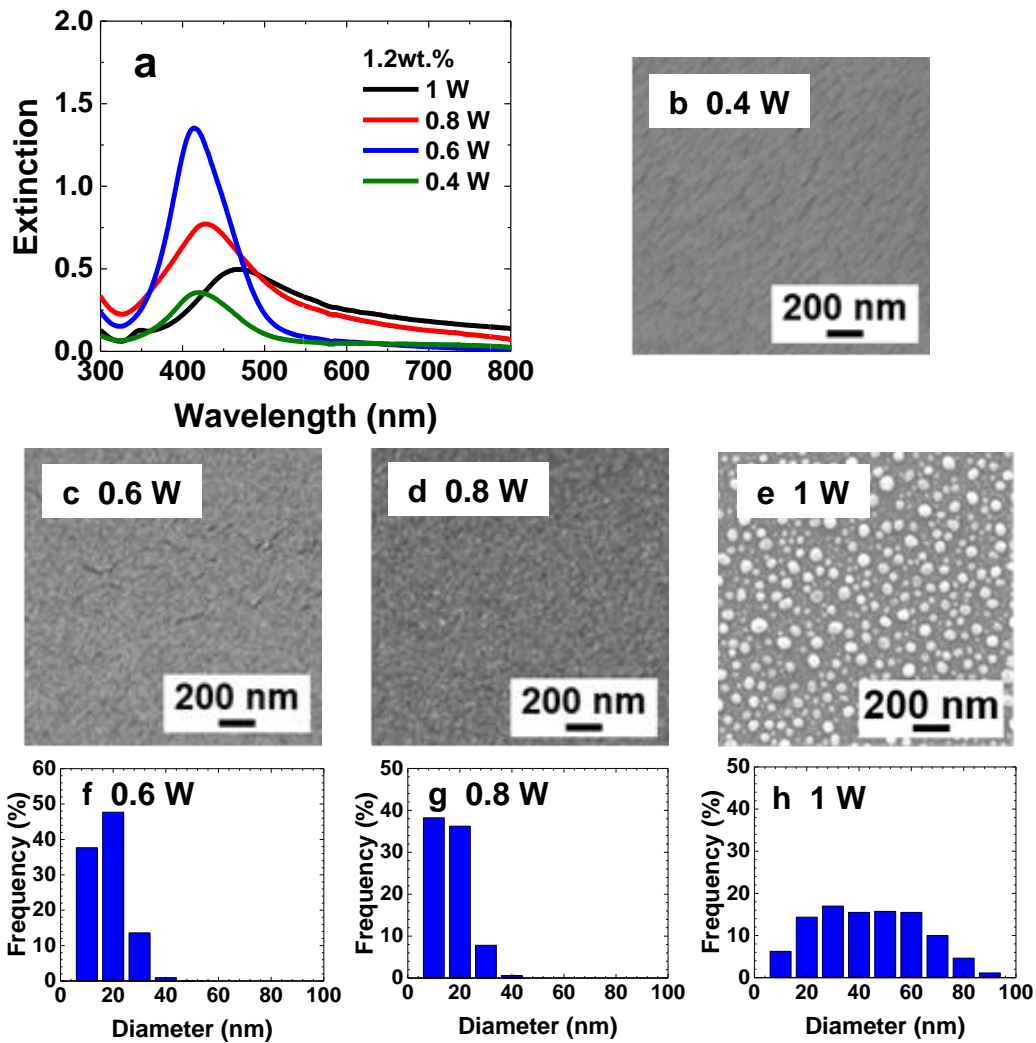


Fig. 5 (a) UV-Vis spectra, (b-e) SEM images, (f-h) histograms of nanoparticle size distribution of the Ag(1.2 wt.%) - PVA films for different laser powers. The irradiation time is 1200 sec for all cases.

PVA solution with more diluted 1.2 wt% concentration of AgNO_3 , and synthesize the Ag(1.2 wt.%) - PVA films by the 1200 sec irradiation at the relatively low laser power, 0.4-0.8 W. The results are summarized in Fig. 5. Although we can observe the small peak of SPR at the laser power of 0.4 W (Fig. 5a), Ag NPs are not visible in the SEM image (Fig. 5b), which means that the synthesized Ag NPs are too small to detect with the resolution of our SEM. The reason for this would be that, due to the low film temperature of 80 °C at 0.4 W (Fig. 1), the synthesized seed Ag NPs cannot diffuse even for a short distance to meet other seed Ag NPs to merge to form larger Ag NPs. As the laser power increases the size of Ag NPs grows (Figs. 5c-h) and the SPR becomes broader (Fig. 5a) with some red shift, which resembles the case of conventional thermal annealing [17] and CW laser annealing with a visible laser

[35]. Under the same irradiation condition of 1200 sec at 1 W, the degree of aggregation of the Ag(1.2 wt.%) -PVA film (Fig. 5a, e, h) is much less compared with that of the Ag(4.9 wt.%) -PVA film (Fig. 3a, c, f), because the number of AgNPs in the former film is much less to aggregate. Consistently, at the lower laser power of 0.4 and 0.6 W, the synthesized Ag(1.2 wt.%) -PVA films after the 1200 sec irradiation at 0.4 and 0.6 W are practically free from aggregation, which is obvious from the absence of the tails in the corresponding SPR spectra (green and blue curves in Fig. 5a).

Now, we choose the laser power of 0.5 W with the irradiation time of 10-1200 sec, and synthesize the Ag(1.2, 2.4, and 4.9 wt.%) -PVA films. The UV-vis spectra of the synthesized Ag(1.2, 2.4, and 4.9 wt.%) -PVA films are shown in Fig. 6. Unlike the Ag(1.2, 2.4, and 4.9 wt.%) -PVA films synthesized at the laser power of 1 W (Fig. 2) the 10 sec irradiation at 0.5 W does not result in the visible SPR in the UV-vis spectra for all three concentrations (Figs. 6a-c), because the reduction goes very slow at this laser power and hence film temperature. Of course, after the longer irradiation, say, 120 sec, the SPR becomes visible at all concentrations. Although Fig. 4 has already shown that aggregation of Ag NPs can be effectively avoided at the laser power of 0.5 W for the concentration of 4.9 wt.% (and obviously below 4.9 wt.% as well), this does not necessarily mean that the size of synthesized Ag NPs under this condition are uniform, since the widths of SPRs we see in Figs. 6a-c are not very narrow. In contrast, the widths of SPRs we see in Figs. 2a-b after the 10 sec irradiation at 1 W are narrower for all three concentrations of AgNO₃. From the results at 1 W (Fig. 2) and 0.5 W (Fig. 6) with three different concentrations of AgNO₃ we can confirm that not only the laser power and irradiation time but also the concentration of NPs precursor (AgNO₃ in this study) strongly influence the size and size distribution (and hence the peak position and width of SPR) of synthesized NPs in the polymer matrix. The use of digestive ripening process [36] may be one way, if necessary, to improve the dispersity of size distribution.

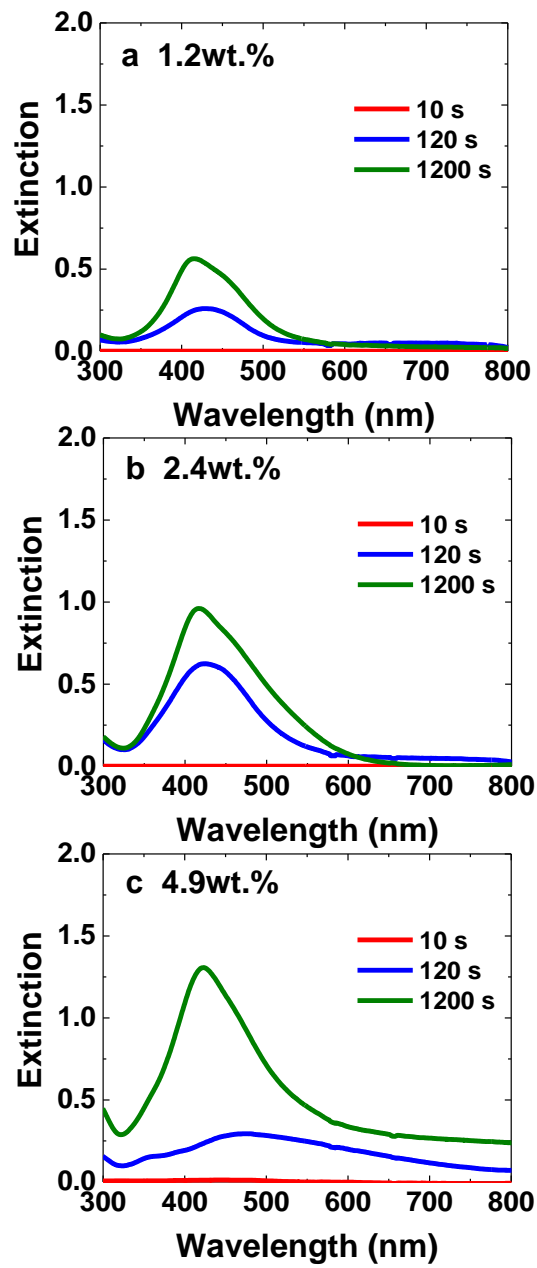


Fig. 6 Similar to Fig. 2 but at the laser power of 0.5 W.

Conclusion

In conclusion we have studied the optical and morphological properties of metal-polymer (Ag-PVA) nanocomposite films synthesized by the irradiation of CO₂ laser with the laser power, irradiation time, and concentration of nanoparticle precursor being the controlled parameters. We have found that all those three factors influence the nanoparticle size and size distribution, and accordingly the position and width of surface plasmon resonance. The use of high laser power is very convenient to quickly (within a few seconds) synthesize nanoparticles in the polymer matrix, but the irradiation time and the concentration of nanoparticle precursor have to be carefully chosen. Otherwise severe aggregation can take place. We have found two approaches to synthesize relatively small metal NPs without severe aggregation. One is to set the laser power low and the other is to employ the low concentration of nanoparticle precursor. Our findings indicate that the size and size distribution of metal nanoparticles can be well-controlled by the choice of CO₂ laser power, irradiation time, and concentration of nanoparticle precursor.

Acknowledgements

This work was supported by a Grant-in-Aid for scientific research from the Ministry of Education, Culture, Sports, Science and Technology (Japan).

References

1. Sih BC, Wolf MO (2005) Metal nanoparticle - Conjugated polymer nanocomposites. *Chem Commun* 3375–3384. <https://doi.org/10.1039/b501448d>
2. Jain PK, Huang X, El-sayed IH, El-sayed MA (2008) Noble Metals on the Nanoscale: Optical and Photothermal Properties and Some Applications. *Acc Chem Res* 41:7–9. <https://doi.org/10.1021/ar7002804>
3. Ramesh G V., Porel S, Radhakrishnan TP (2009) Polymer thin films embedded with in situ grown metal nanoparticles. *Chem Soc Rev* 38:2646–2656. <https://doi.org/10.1039/b815242j>
4. Faupel F, Zaporojtchenko V, Strunskus T, Elbahri M (2010) Metal-polymer nanocomposites for functional applications. *Adv Eng Mater* 12:1177–1190. <https://doi.org/10.1002/adem.201000231>
5. Mir SH, Nagahara LA, Thundat T, et al (2018) Review—Organic-Inorganic Hybrid Functional Materials: An Integrated Platform for Applied Technologies. *J Electrochem Soc* 165:B3137–B3156. <https://doi.org/10.1149/2.0191808jes>
6. Mbhele ZH, Salemane MG, Sittert CGCE Van, et al (2003) Fabrication and Characterization of Silver - Polyvinyl Alcohol Nanocomposites. *Chem Mater* 15:5019–5024
7. Khanna PK, Singh N, Charan S, et al (2005) Synthesis and characterization of Ag/PVA nanocomposite by chemical reduction method. *Mater Chem Phys* 93:117–121. <https://doi.org/10.1016/j.matchemphys.2005.02.029>
8. Xu P, Han X, Zhang B, et al (2014) Multifunctional polymer-metal nanocomposites via direct chemical reduction by conjugated polymers. *Chem Soc Rev* 43:1349–1360. <https://doi.org/10.1039/c3cs60380f>
9. Korchev AS, Bozack MJ, Slaten BL, Mills G (2004) Polymer-Initiated Photogeneration of Silver Nanoparticles in SPEEK/PVA Films: Direct Metal Photopatterning. *J Am Chem Soc* 126:10–11. <https://doi.org/10.1021/ja037933q>
10. Sakamoto M, Tachikawa T, Fujitsuka M, Majima T (2006) Acceleration of Laser-Induced Formation of

Gold Nanoparticles in a Poly (vinyl alcohol) Film. *Langmuir* 22:6361–6366

11. Pucci A, Bernabò M, Elvati P, et al (2006) Photoinduced formation of gold nanoparticles into vinyl alcohol based polymers. *J Mater Chem* 16:1058–1066. <https://doi.org/10.1039/b511198f>
12. Sakamoto M, Tachikawa T, Fujitsuka M, Majima T (2007) Photochemical formation of Au/Cu bimetallic nanoparticles with different shapes and sizes in a poly(vinyl alcohol) film. *Adv Funct Mater* 17:857–862. <https://doi.org/10.1002/adfm.200600700>
13. Lee CJ, Karim MR, Lee MS (2007) Synthesis and characterization of silver/thiophene nanocomposites by UV-irradiation method. *Mater Lett* 61:2675–2678. <https://doi.org/10.1016/j.matlet.2006.10.021>
14. Jiang T, Li J, Zhang L, et al (2014) Microwave assisted in situ synthesis of Ag-NaCMC films and their reproducible surface-enhanced Raman scattering signals. *J Alloys Compd* 602:94–100
15. Porel S, Singh S, Harsha SS, et al (2005) Nanoparticle-embedded polymer: In situ synthesis, free-standing films with highly monodisperse silver nanoparticles and optical limiting. *Chem Mater* 17:9–12. <https://doi.org/10.1021/cm0485963>
16. Karthikeyan B, Anija M, Phillip R (2006) In situ synthesis and nonlinear optical properties of Au:Ag nanocomposite polymer films. *Appl Phys Lett* 88:053104. <https://doi.org/10.1063/1.2168667>
17. Gradess R, Abargues R, Habbou A, et al (2009) Localized surface plasmon resonance sensor based on Ag-PVA nanocomposite thin films. *J Mater Chem* 19:9233–9240. <https://doi.org/10.1039/b910020b>
18. Hariprasad E, Radhakrishnan TP (2013) In situ fabricated polymer-silver nanocomposite thin film as an inexpensive and efficient substrate for surface-enhanced raman scattering. *Langmuir* 29:13050–13057. <https://doi.org/10.1021/la402594j>
19. Elashmawi IS, Menazea AA (2019) Different time ' s Nd : YAG laser-irradiated PVA / Ag nanocomposites : structural , optical , and electrical. *J Mater Res Technol* 8:1944–1951
20. Kashihara K, Uto Y, Nakajima T (2018) Rapid in situ synthesis of polymer-metal nanocomposite films in

- several seconds using a CO₂ laser. *Sci Rep* 8:14719. <https://doi.org/10.1038/s41598-018-33006-9>
21. Nishikawa H, Nakata E, Nakano S, et al (2019) Influence of polymer molecular weight on the properties of in situ synthesized silver – methylcellulose nanocomposite films with a CO₂ laser. *J Mater Sci* 55:2090–2100. <https://doi.org/10.1007/s10853-019-04149-5>
 22. Maurya SK, Uto Y, Kashihara K, et al (2018) Rapid formation of nanostructures in Au films using a CO₂ laser. *Appl Surf Sci* 427:961–965. <https://doi.org/10.1016/j.apsusc.2017.09.044>
 23. Faniayeu I, Ishimatsu Y, Nakajima T (2019) Surface plasmon resonance tuning of Ag nanoisland films using a CO₂ laser. *J Phys D Appl Phys* 52:1–8. <https://doi.org/10.1088/1361-6463/ab1b7b>
 24. Chen C, Li J, Luo G, et al (2012) Size-controlled in situ synthesis and photo-responsive properties of silver/poly(methyl methacrylate) nanocomposite films with high silver content. *Appl Surf Sci* 258:10180–10184. <https://doi.org/10.1016/j.apsusc.2012.06.102>
 25. Abyaneh MK, Paramanik D, Varma S, et al (2007) Formation of gold nanoparticles in polymethylmethacrylate by UV irradiation. *J Phys D Appl Phys* 40:3771–3779. <https://doi.org/10.1088/0022-3727/40/12/032>
 26. Spano F, Massaro A, Blasi L, et al (2012) In situ formation and size control of gold nanoparticles into chitosan for nanocomposite surfaces with tailored wettability. *Langmuir* 28:3911–3917. <https://doi.org/10.1021/la203893h>
 27. Torrell M, Cunha L, Cavaleiro A, et al (2010) Functional and optical properties of Au:TiO₂ nanocomposite films: The influence of thermal annealing. *Appl Surf Sci* 256:6536–6542. <https://doi.org/10.1016/j.apsusc.2010.04.043>
 28. Torrell M, Kabir R, Cunha L, et al (2011) Tuning of the surface plasmon resonance in TiO₂/Au thin films grown by magnetron sputtering: The effect of thermal annealing. *J Appl Phys* 109:1–9. <https://doi.org/10.1063/1.3565066>

29. Takele H, Greve H, Pochstein C, et al (2006) Plasmonic properties of Ag nanoclusters in various polymer matrices. *Nanotechnology* 17:3499–3505. <https://doi.org/10.1088/0957-4484/17/14/023>
30. Takele H, Jebril S, Strunskus T, et al (2008) Tuning of electrical and structural properties of metal-polymer nanocomposite films prepared by co-evaporation technique. *Appl Phys A Mater Sci Process* 92:345–350. <https://doi.org/10.1007/s00339-008-4524-0>
31. Beyene HT, Chakravadhanula VSK, Hanisch C, et al (2010) Preparation and plasmonic properties of polymer-based composites containing Ag-Au alloy nanoparticles produced by vapor phase co-deposition. *J Mater Sci* 45:5865–5871. <https://doi.org/10.1007/s10853-010-4663-5>
32. Schürmann U, Hartung W, Takele H, et al (2005) Controlled syntheses of Ag-polytetrafluoroethylene nanocomposite thin films by co-sputtering from two magnetron sources. *Nanotechnology* 16:1078–1082. <https://doi.org/10.1088/0957-4484/16/8/014>
33. Avasthi DK, Mishra YK, Kabiraj D, et al (2007) Synthesis of metal-polymer nanocomposite for optical applications. *Nanotechnology* 18:. <https://doi.org/10.1088/0957-4484/18/12/125604>
34. Hourd AC, Baker RT, Abdolvand A (2015) Structural characterisation of printable noble metal/poly(vinyl-alcohol) nanocomposites for optical applications. *Nanoscale* 7:13537–13546. <https://doi.org/10.1039/c5nr03636d>
35. Paeng D, Lee D, Grigoropoulos CP (2014) Characteristic time scales of coalescence of silver nanocomposite and nanoparticle films induced by continuous wave laser irradiation. *Appl Phys Lett* 105:1–5. <https://doi.org/10.1063/1.4893465>
36. Sahu P, Prasad BLV (2013) Fine control of nanoparticle sizes and size distributions: Temperature and ligand effects on the digestive ripening process. *Nanoscale* 5:1768–1771. <https://doi.org/10.1039/c2nr32855k>